Transactions of the **13th International Conference on Structural Mechanics in Reactor Technology** (SMiRT 13), Escola de Engenharia - Universidade Federal do Rio Grande do Sul, Porto Alegre, Brazil, August 13-18, 1995

Shock waves in concrete - constitutive laws

Eibl, J., Ockert, J.
University of Karlsruhe, Inst. für Massivbau und Baustofftechnologie, Karlsruhe, Germany

1. INTRODUCTION

The analysis of shock wave is required designing concrete structures against explosion, detonation and impact loading. In the past such types of analysis were only of interest for military purposes but meanwhile more and more civil applications arise in traffic and industrial facilities.
Finite Element Codes - usually so-called Hydrocodes - are needed to analyze these complex loading cases for different materials. To describe the interesting response behavior realistic constitutive models $\sigma_{ij} = f(D_{ij},E)$ are needed, which until now are not available in a sufficient verified form.
Therefore attempts were made in the last years by several scientists to obtain resp. verify corresponding constitutive laws ([1], [4]).
In the following a report sponsored by BMFT [5] on shock wave experiments is given which are used to determine the hydrostatic part of such a model. The deviatoric part is estimated in a first approach by some reanalysis of the tests using an existing computer code for shock wave analysis.

2. THEORETICAL BACKGROUND

The formation of shock waves is simply shown starting from the one-dimensional wave equation for a nonlinear constitutive relation:

$$\frac{\partial^2 u}{\partial t^2} = c^2 \frac{\partial^2 u}{\partial x^2} \quad , \tag{1}$$

with

$$c = \sqrt{\frac{H}{\varrho}} \quad . \tag{2}$$

Here c is the propagation velocity of the wave and $H = d\sigma/d\varepsilon$ is the slope of the nonlinear stress strain relationship. If the slope increase with increasing stress then parts of the wave with higher stress magnitude travels faster than parts with lower stresses (s.

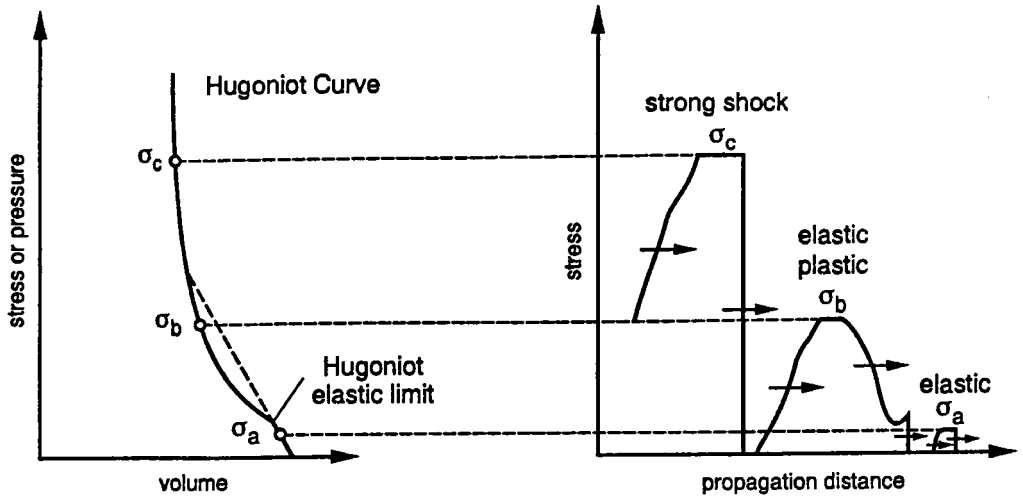

Fig. 1 Formation of shock waves in solids

fig 1). The wave front steeps up and the propagation velocity is greater than the sound velocity. This type of wave is called shock wave and the resulting magnitude of pressure is much higher than the one-dimensional strength of the material.

If the magnitude of such a shock greatly exceeds the maximum shear stress that a material can sustain, the difference between the principal stress components and the hydrostatic pressure within the material are small, that the shear stresses may be neglected and the response of a solid may be reduced to that of an inviscid fluid [4]. Therefore in all typical experiments to study the relation between hydrostatic pressure and volume only plane waves are generated simplifying the problem to a one-dimensional flow problem. Then conservation laws of mass, momentum and energy may be written as follows (fig. 2):

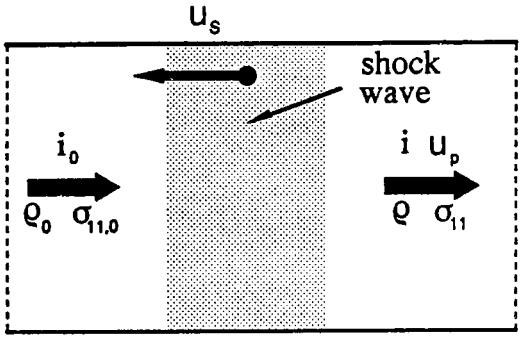

Fig. 2 Shock wave in one-dimensional flow

$$\begin{aligned} \varrho\cdot(U_s-u_p) &= \varrho_0\cdot U_s && \text{Conservation of mass} \\ p+\varrho\cdot(U_s-u_p)^2 &= p_0+\varrho_0\cdot U_s^2 && \text{Conservation of momentum} \\ i+\frac{1}{2}\cdot(U_s-u_p)^2 &= i_0+\frac{1}{2}\cdot U_s^2 && \text{Conservation of energy} \end{aligned} \qquad (3)$$

Considering that the initial variables i_0, p_0 and ϱ_0 of the material into which the shock propagates are known, there remain 5 variables:

shock wave velocity U_s	density ϱ
particle velocity u_p	pressure p
enthalpy $i = E + pV$.	

If the boundary pressure p is known, the conservation laws give three relations for the remaining 4 variables. Therefore one additional relationship is needed. This is the so-called Hugoniot Curve which reflects the material behavior (fig. 3). It represents the

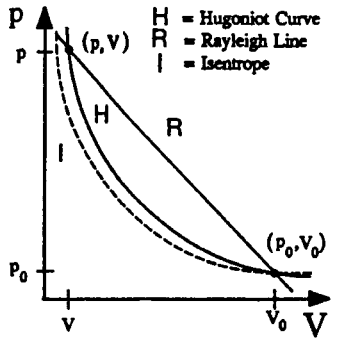

Fig. 3 Hugoniot Curve, Rayleigh Line and Isentrope for an inviscid fluid

sum of all end states (p,V) that can be reached from the initial state (p_0,V_0) via a straight line, the so-called Rayleigh Line. The slope of this line can be obtained from conservation of mass and momentum (see eq. 3):

$$\frac{p-p_0}{V_0-V} = \left(\frac{U_s}{V_0}\right)^2 \qquad (4)$$

The Hugoniot Curve is only one part of the needed Equation of State (EOS). It represents a line of a three-dimensional surface in the p-V-E coordinate system. An additional assumption is needed to extend the measured Hugoniot Curve to a complete EOS. This is usually done with the Mie-Grüneisen EOS:

$$p(V,E) = p_{0K} + \frac{\gamma(V)}{V}\cdot[E-E_{0K}] \quad , \qquad (5)$$

where γ is the Grüneisen parameter, for which different formulations have been proposed in the past. A third order differential equation arises from inserting these formulations into the EOS. A program was written to solve this equation numerically. The results are the energy $E_{0K} = f(V)$, pressure $p_{0K} = f(V)$ and bulk modul $K_{0K} = f(V)$. In addition the temperature along the Hugoniot Curve and any isotherm can be produced. In the calculation the porosity of concrete was considered [5].

3. SHOCK WAVE EXPERIMENTS

First shock wave experiments were carried out to determine the hydrostatic part of the constitutive model. The test setup with quadratic concrete slabs 100 × 100 × 25 cm is shown in fig. 4. The explosive charge is placed at the center of the surface of the slab. Several gauges, Hot-Molded Carbon Composition resistors, are located directly underneath the charge to measure the compressive shock wave. Changes in resistance at each gauge are determined by measuring the voltage output during the test. Using a calibration curve for the resistors, this output is transformed into pressure values. The shock wave velocity can be calculated from the arrival time of the wave at each location, if the distance between the gauges is known. Using eq. 4 one point of the Hugoniot Curve for each gauge can be determined.

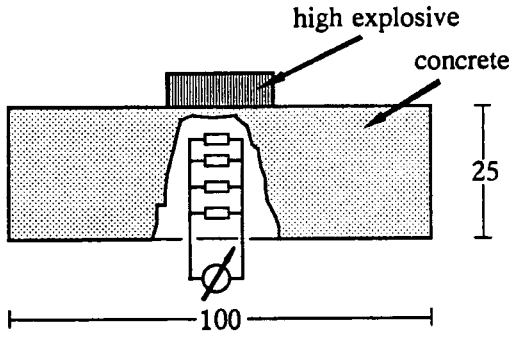

Fig. 4 Experimental Setup

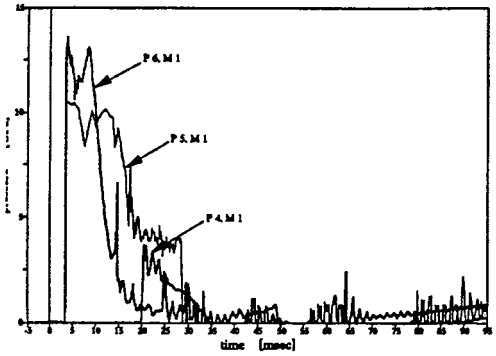

Fig. 5 Pressure-time history

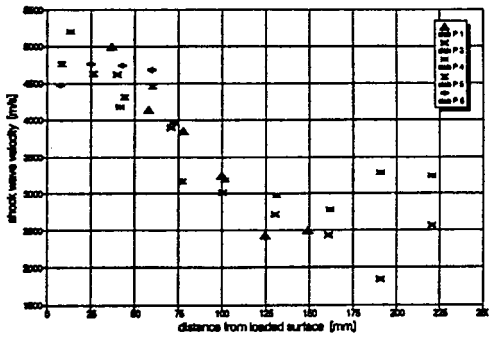

Fig. 6 Measured shock wave velocities

In this research program 8 tests with different geometries were carried out. The maximum measured pressure magnitude was 13,5 GPa (s. fig 5). Such high magnitudes exist only directly under the loaded surface of the slab. With increasing distance from this surface the pressure magnitude decrease rapidly. The shock wave velocities obtained in the tests were shown in fig. 6. The maximum shock wave velocity was about 5000 m/s and so significantly faster than the velocity of sound for concrete (≈ 3800 m/s). Additional wave velocities have been measured, that are below the velocity of sound (s. fig. 6). Fig. 7 shows the resulting Hugoniot Curve together with first experiments of Grady [6] and Gregson [7] using very smal size specimens.

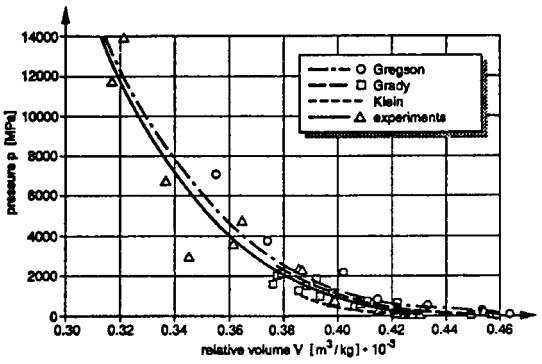

Fig. 7 Hugoniot Curve of concrete

4. RESULTS

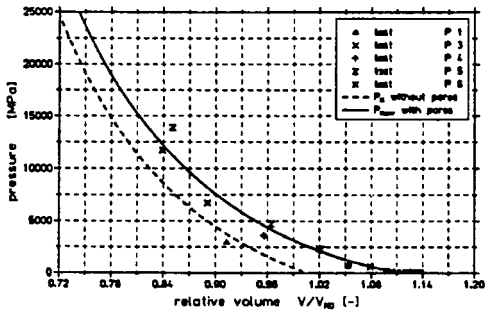

Fig. 8 Results of calculation

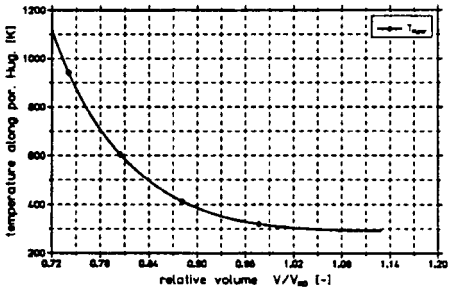

Fig. 9 Temperature along Hugoniot Curve

Starting from the Mie-Grüneisen EOS, as mentioned in chapter 2, a third order differential equation was obtained. For more details see [5]. Together with the experimental determined Hugoniot Curve and a function of specific heat at constant volume C_V (s.

[5]) eq. 7 could be solved numerically. The porosity of concrete was taken into consideration through the p-α model after Herrmann [8]. The result of this calculation fits the experimental values very well (s. fig. 8). The temperature following from shock wave loading is plotted in fig. 9. Compared with fig. 8 one can see that the maximum temperature difference obtained in the tests was approximate 250°K. This difference only results from the compaction process and not from the heat of the high explosive.

5. FINITE ELEMENT CALCULATIONS

For an accurate reanalysis of the tests not only the concrete slab was modeled with Finite Elements but also the high explosive charge. So the interaction between high explosive and concrete can be considered which is otherwise impossible. The resulting pressure and volume changes are determined by means of the EOS from Jones, Wilkins and Lee [2]:

$$p(V,E) = A\cdot(1-\frac{\omega}{R_1\cdot V})\cdot e^{-R_1 V} + B\cdot(1-\frac{\omega}{R_2\cdot V})\cdot e^{-R_2 V} + \frac{\omega\cdot E}{V} \quad , \qquad (6)$$

where the constants A,B,R_1,R_2 and ω depend from the type of explosive used.

For concrete a constitutive model from Finite Element Code DYNA2D [9] was used. It is split into two parts, the hydrostatic part and the deviatoric part. For the hydrostatic part the following EOS was used:

$$p = C(\varepsilon_v) + \gamma\cdot D(\varepsilon_v)\cdot E \quad . \qquad (7)$$

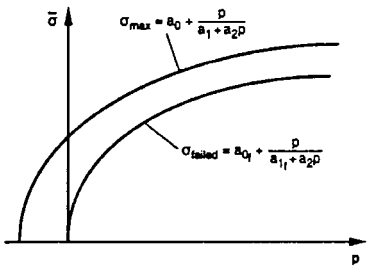

Fig. 10 Failure surface

The input parameters were chosen to match the Mie-Grüneisen EOS from chapter 4. The failure surface of this model is shown in fig. 10. A damage function $\eta = f(\xi)$ is used to move from σ_{max} in fig. 10 to σ_{failed}. The influence of strain rate was modelled after [3].
For the reanalysis of test 3 a finite element mesh was used that contains about 7000 twodimensional axissymmetric elements, the high explosive elements being much smaller than the concrete elements. Between the high explosive and the concrete slab a slide line was defined. The ignition was initiated at top of the charge as in the tests. The profile of maximum pressure in each element is shown in fig. 11. Similar to the tests the pressure rapidly decreases with increasing distance from loaded surface. Fig. 12 gives the axial strain together with the deformed geometry after 3000 µsec, showing a big crater which in the meantime has developed, while the center of the slab is strongly deformed. The region with the bright color indicates that most of the slab is damaged in tension. This is similar to the experiment.

6. SUMMARY AND CONCLUSION

A constitutive law was developed for concrete as a basis for research on shock loading. Therefore the Hugoniot Curve of concrete was established up to 13.5 GPa in experiments. With the theories of Mie-Grüneisen and Debeye the Hugoniot Curve was extend-

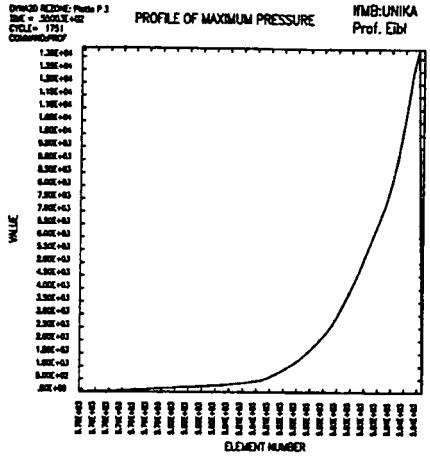

Fig. 11 Profile of maximum pressure

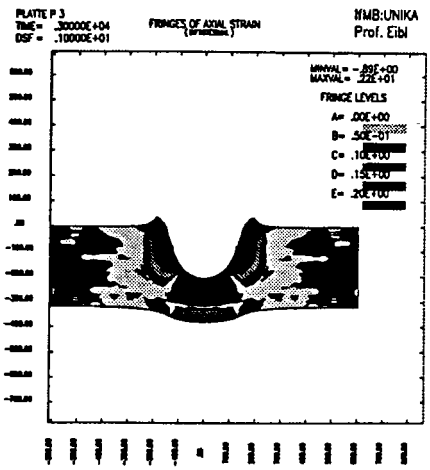

Fig. 12 Deformed geometrie

ed to a complete Mie-Grüneisen EOS.
In addition the energy, pressure and bulk modul of 0°K Isotherm and the temperature along the Hugoniot Curve were received. Furtherone any isotherm or isentrope could be calculated.
The results were controlled by a finite element analysis where the high explosive was modelled with finite elements. The numerical results match the experiments very well.

REFERENCES

[1] Anderson, C. E. JR, Bodner, S. R.: "Ballistic impact: The status of analytical and numerical modeling", *Int. J. Impact Engng. 7 (1988)*, pp. 9-35

[2] Dobratz, B. M.: *LLNL Explosives Handbook: Properties of chemical explosives and explosive simulants*, Lawrence Livermore National Laboratory, UCRL-52997, 1981

[3] Eibl, J., et. al.: *Concrete Structures under Impact and Impulsive Loading*. Bulletin d'Information, No. 187, CEB, 1988

[4] Eibl, J., Henseleit, O., Schlüter, F.-H.: "Baudynamik", *Beton-Kalender 1988*, Ernst & Sohn, pp. 665-774

[5] Eibl, J., Ockert, J.: *Stoffgesetzliche Grundlagen für die Schockwellenausbreitung im Beton*, Abschlußbericht, Institut für Massivbau und Baustofftechnologie, Abteilung Massivbau, Universität Karlsruhe, 1994

[6] Grady, D. E.: *Impact Compression Properties of Concrete*, Sixth International Symposium on Interaction of Nonnuclear Munitions with Structures, Panama City Beach, Florida, 1993

[7] Gregson, V. R., Jr.: *A Shock Wave Study of Fondu-Fyre WA-1 and Concrete*, General Motors Materials and Structures Laboratory, Report MSL-70-30, 1971

[8] Herrmann, W.: "Constitutive Equation for the Dynamic Compaction of Ductile Porous Materials", *J. Appl. Phys.*, Vol 40, No. 6, 1969, pp. 2490-2499

[9] Whirley, R. G., Engelmann, B. E.: *DYNA2D: A nonlinear, explicit, two-dimensional finite element code for solid mechanics. User Manual*, Lawrence Livermore National Laboratory, UCRL-MA-110630, 1992